

# Fault-tolerant Quantum Communication Based on Solid-state Photon Emitters

L. Childress,<sup>1</sup> J. M. Taylor,<sup>1</sup> A. S. Sørensen,<sup>1,2,3</sup> and M. D. Lukin<sup>1,2</sup>

<sup>1</sup>*Department of Physics, Harvard University, Cambridge, Massachusetts, 02138*

<sup>2</sup>*ITAMP, Harvard-Smithsonian Center for Astrophysics, Cambridge, Massachusetts, 02138*

<sup>3</sup>*The Niels Bohr Institute, University of Copenhagen, DK-2100 Copenhagen Ø, Denmark*

(Dated: February 9, 2020)

We describe a novel method for long distance quantum communication in realistic, lossy photonic channels. The method uses single emitters of light as intermediate nodes in the channel. One electronic spin and one nuclear spin degree of freedom associated with each emitter provide quantum memory and enable active error correction. We show that these two degrees of freedom, coupled via the contact hyperfine interaction, suffice to correct arbitrary errors, making our protocol robust to all realistic sources of decoherence. The method is particularly well suited for implementation using recently-developed solid-state nano-photonic devices.

PACS numbers: 03.67.Hk, 03.67.Mn, 78.67.Hc

Quantum communication holds promise for transmitting secure messages via quantum cryptography, and for distributing quantum information [1]. However, attenuation in optical fibers fundamentally limits the range of direct quantum communication techniques [2], and extending them to long distances remains a conceptual and technological challenge. In principle, photon losses can be overcome by introducing intermediate quantum nodes and utilizing a so-called quantum repeater protocol [3]. Such a repeater creates quantum entanglement over long distances by building a backbone of entangled pairs between closely-spaced nodes. Performing an entanglement connection at each intermediate node [4] leaves the outer two nodes entangled, and this long-distance entanglement can be used to teleport quantum information [5, 6] or transmit secret messages via quantum key distribution [7]. Even though quantum operations are subject to errors, by incorporating entanglement purification [8, 9] at each step, one can extend entanglement generation to arbitrary distances without loss of fidelity in a time that scales polynomially with distance [3]. This should be compared to direct communication which scales exponentially making it intractable for long distances. While approaches to quantum repeaters based many quantum bits (qubits) at each node [10, 11] or on photon storage in atomic ensembles [12] are now being actively explored, realization of a robust, practical system that can tolerate all expected errors remains a difficult task.

In this Letter, we propose a quantum repeater in which each node is formed by a single quantum emitter with two internal degrees of freedom (Figure 1a). Specifically, we consider emitters with a pair of electronic spin sublevels that allows for spin-selective optical excitation, and a proximal nuclear spin provides an auxiliary memory. Although our approach is relevant to atomic systems, such as single atoms trapped in a cavity [13] or single trapped ions [10], it is particularly suitable for implementation with solid-state emitters, for example impurity color centers [14, 15] and quantum dots [16, 17]. These devices of

fer many attractive features including optically accessible electronic and nuclear spin degrees of freedom, potential opto-electronic integrability, and fast operation.

The initial step in our scheme is entanglement generation between two emitters separated by a distance  $L_0$ . In principle, entanglement can be generated probabilistically by a variety of means, e.g., Raman scattering [18] or polarization-dependent fluorescence [10]. However, solid-state emitters often do not exhibit appropriate selection rules, and for our repeater protocol it is essential that the optical transition be independent of the nuclear spin state. For these reasons, we consider an entanglement mechanism based on state-selective elastic light scattering as shown in Figure 1. Elastic light scattering places few restrictions on selection rules, and permits nuclear-spin-independent fluorescence as we discuss below.

To implement the entanglement scheme, each emitter is placed inside a photonic cavity to increase collection efficiency, and the cavity output is coupled to a single-mode photonic fiber. The optical transition frequencies in each node can be matched by careful selection or tuning of the emitters. Two adjacent repeater nodes form state-selective mirrors in an interferometer, such that each node scatters light only if its electron spin is in state  $|0\rangle$ . If the interferometer is properly balanced (using, for example, auxiliary laser pulses or a plug-and-play system analogous to that used in quantum key distribution [19]), then when both nodes are in the scattering state  $|0\rangle$  the outgoing photons will always exit one detector arm  $D_+$ . Consequently, a detection event in the other arm  $D_-$  must correspond to scattering by only one of the two nodes; since the photon could have scattered off either node, the  $D_-$  measurement can project the nodal spins onto an entangled state.

Specifically, we assume that each node is prepared in a superposition state  $(|0\rangle + |1\rangle)/\sqrt{2}$ , where only state  $|0\rangle$  is coupled to an excited level, which decay with a rate  $\gamma$ . In the weak excitation limit, we can adiabatically eliminate the excited state, and the light scattered off state  $|0\rangle$  is

well described as a coherent state. The combined state of node  $i$  and the scattered light field is then given by  $|\psi\rangle_i \approx (|1\rangle + T_i |0\rangle)/\sqrt{2}$  with

$$T_i = \exp[-\sqrt{P_{\text{em}}}(\sqrt{1-\epsilon}\hat{b}_i^\dagger + \sqrt{\epsilon}\hat{a}_i^\dagger) - P_{\text{em}}/2], \quad (1)$$

where  $P_{\text{em}}$  is the total emission probability,  $\epsilon$  comprises the net collection, propagation, and detection efficiency, and  $\hat{a}_i, \hat{b}_i$  are the annihilation operators for the field reaching the beam splitter and other (loss) fields, respectively. Provided that  $P_{\text{em}} \ll 1$ , a detection event in detector  $D_-$  (mode  $\hat{d}_- \propto \hat{a}_1 - \hat{a}_2$ ) projects the system onto a maximally entangled state  $\hat{d}_-(T_1 |01\rangle + T_2 |10\rangle)/2 \propto (|01\rangle - |10\rangle)/\sqrt{2} = |\Psi_-\rangle$ . For finite  $P_{\text{em}}$ , there is a chance  $\sim P_{\text{em}}$  that, during a successful  $D_-$  detection event, an additional photon was emitted into the environment. Since the  $|00\rangle$  and  $|11\rangle$  states do not produce clicks in  $D_-$ , this will mainly result in some admixture of the state  $|\Psi_+\rangle = (|0\rangle|1\rangle + |1\rangle|0\rangle)/\sqrt{2}$ , which we refer to as a phase error. Another source of error is the homogeneous broadening typically found in solid-state emitters. We model this dephasing by a random energy shift of the excited state  $\Delta$  with white-noise characteristics ( $\langle \Delta(t)\Delta(t') \rangle = \Gamma\delta(t-t')$ ). Solving the Heisenberg equations for an emitter coupled to an optical cavity with vacuum Rabi coupling  $g$  and linewidth  $\kappa$ , and averaging over the noise, we obtain the associated fidelity loss [20]. Putting these considerations together, we find that the entanglement scheme succeeds with probability  $P = (1/2)(1 - e^{-P_{\text{em}}\epsilon/2}) \approx \epsilon P_{\text{em}}/4$ , producing the state  $|\Psi_-\rangle$  in time  $T_0 \approx (t_0 + t_c)/P$  with fidelity

$$F_0 = \frac{1}{2} \left( 1 + e^{-P_{\text{em}}(1-\epsilon)} \right) - \gamma_e(t_0 + t_c) - \gamma_{dc} \frac{t_0}{P} - \frac{3}{2} \frac{\Gamma}{\Gamma + \gamma} \frac{\kappa}{\kappa + \gamma} \frac{1}{1 + 4g^2/\kappa(\gamma + \Gamma)}. \quad (2)$$

Here, the first term can be derived from Eq. (1); the second term accounts for electron spin dephasing (at rate  $\gamma_e$ ) during the time required for excitation  $t_0$  and classical communication  $t_c$ ; the third term accounts for detector dark counts at rate  $\gamma_{dc}$ ; the last term arises from homogeneous broadening. For realistic emitters placed into a cavity with either a narrow linewidth  $\kappa \ll \gamma$  or a modest Purcell factor  $4g^2/(\kappa(\gamma + \Gamma)) > 1$ , the first two terms should dominate the error. Both of these contributions introduce phase errors.

Using this procedure, electron spin entanglement can be generated between pairs of nodes. The electron spin state is then mapped onto the auxiliary nuclear spin qubit for long-term storage using the hyperfine interaction, leaving the electronic degree of freedom available to generate entanglement between unconnected nodes, as illustrated in Figure 1b. Due to a large difference in electronic and nuclear magnetic moments hyperfine coupling can be turned on and off by pulsed magnetic fields. By combining optical detection of individual electron spin states [21] and effective two-qubit operations

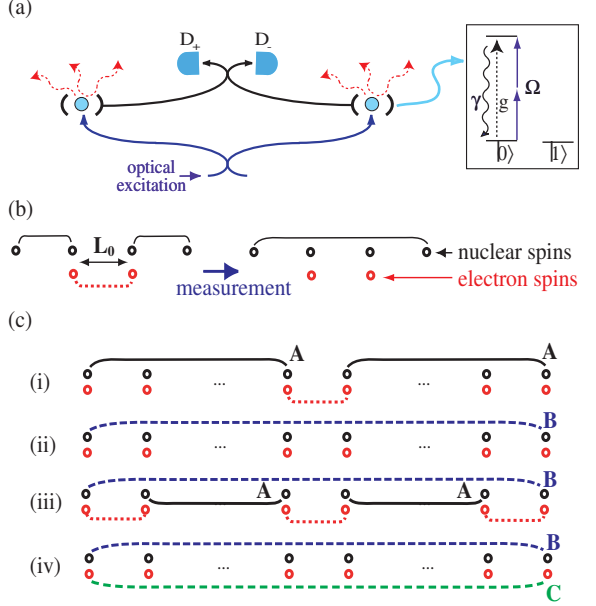


FIG. 1: Protocol for fault-tolerant quantum communication. (a) Interferometric arrangement for entanglement generation. Inset shows relevant level scheme. (b) Entanglement propagation by swapping. (c) Nested entanglement purification. Dots indicate an arbitrary number of nodes. (i) We split the set of repeaters in half, create two purified A pairs, and connect them via adjacent central nodes. (ii) This yields an entangled B pair. (iii) While storing the entangled pair in the endpoint stations, we create and purify entangled A pairs using the nearest neighbor and central nodes. (iv) Bell state measurement of the central and nearest neighbor nodes creates a C pair which is used to purify the B pair.

associated with hyperfine coupling of electronic and nuclear spins [22, 23], we may projectively measure all four Bell states in the electronic/nuclear manifold associated with each emitter. The outcomes of the Bell measurements reveal the appropriate local rotations to obtain a singlet state in the remaining pair of nuclear spins, implementing a deterministic entanglement swap [4, 5]. By performing this procedure in parallel, and iterating the process for  $N \propto \log_2(L/L_0)$  layers, we obtain the desired nuclear spin entanglement over distance  $L$  in a time  $\propto L \log_2(L/L_0)$ .

To extend entanglement to long distances in the presence of errors, active purification is required at each level of the repeater scheme. In Figure 1c we present a method which accomplishes this with minimal physical resources at each node. It requires generating an auxiliary entangled electron spin pair (which we label “C”) to purify an entangled pair stored in the nuclear degrees of freedom (“B”). The purification protocol described in [9, 24] is then performed by entangling the electron and nuclear spins via a hyperfine interaction at each node, and subsequently measuring the electron spins. Comparison of the measurement outcomes reveals whether the purification

tion step was successful, resulting in a new stored pair  $B$  with higher fidelity. After successfully repeating the procedure for  $m$  purification steps, the stored pair becomes a purified (“A”) pair, which can then be used to create B and C pairs over longer distances. This procedure is analogous to a pioneering proposal [3]; however, by incorporating two extra connection steps in generating the auxiliary  $C$  pair, the required physical resources are reduced, so that the protocol can be implemented with a single electronic and nuclear spin at each node.

The fidelity obtained at the end of this nested purification procedure,  $F(m, L, F_0, p, \eta)$ , depends on the number of purification steps  $m$ , the distance  $L$  between the outer nodes, the initial fidelity  $F_0$  between adjacent nodes, and the reliability of measurements  $\eta \leq 1$  and local two-qubit operations  $p \leq 1$  required for entanglement purification and connection [24]. As the number of purification steps increases  $m \rightarrow \infty$ , the fidelity at a given distance  $L$  approaches a fixed point  $F \rightarrow F_{FP}(L, F_0, p, \eta)$  at which additional purification steps yield no further benefit [24]. Finally, as  $L$  increases, the fidelity may approach an asymptotic value  $F_{FP} \rightarrow F_\infty(F_0, p, \eta)$ , which is independent of distance [20]. Figure 2a illustrates the efficiency of the purification protocol: for initial fidelities  $F_0 \gtrsim 97\%$ , three purification steps suffice to produce entanglement of large distances. Fig. 2c shows that our scheme will operate in the presence of  $1 - p \lesssim 1\%$  errors in local operations and percent-level phase errors in initial entanglement fidelity. Other types of error are in principle possible. On average, the final fidelity obtained by the nested entanglement purification procedure depends only on the diagonal elements of the density matrix in the Bell state basis  $\{|\Psi_-\rangle, |\Phi_-\rangle, |\Phi_+\rangle, |\Psi_+\rangle\}$ , where  $|\Phi_\pm\rangle = (|0\rangle|0\rangle \pm |1\rangle|1\rangle)/\sqrt{2}$  [9]. We parameterize the initial fidelity by  $\{F_0, (1 - F_0)v, (1 - F_0)v, (1 - F_0)(1 - 2v)\}$  in this basis, so that the shape parameter  $v$  quantifies the weight of non-phase errors. The asymptotic fidelity shown in Fig. 2d for different value of  $v$  indicates that although the protocol we use is most effective for purifying phase errors, it also tolerates arbitrary errors.

Figure 2b demonstrates that our scheme permits generation of high-fidelity, long distance entangled pairs in the presence of percent-level errors in polynomial time. Because solid-state devices allow fast operations and measurements, the overall time scale is set by the classical communication time between nodes. As an example, using a photon loss rate of  $\sim 0.2$  dB/km, nodes separated by  $L_0 \sim 20$  km, an emission probability  $P_{\text{em}} \sim 8\%$ , and just one purification step at each nesting level, our scheme could potentially produce entangled pairs with fidelity  $F \sim 0.8$  sufficient to violate Bell’s inequalities over 1000 km in a few seconds. For comparison, under the same set of assumptions direct entanglement schemes would require  $\sim 10^{10}$  years. Moreover, it is likely that the bit-rate could be significantly improved by employing optimal control theory to tailor the details of the repeater

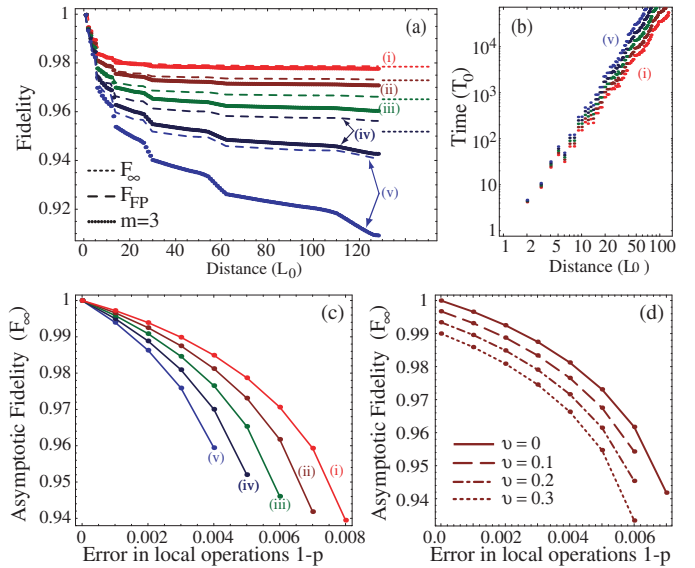


FIG. 2: (a) Fidelity scaling with distance. Points show results using 3 purification steps at each nesting level; dashed lines show the fixed point  $F_{FP}$  at each distance; dotted lines indicate the asymptotic fidelity  $F_\infty$ . For (a) and (b), measurements and local two-qubit operations  $\eta = p$  contain 0.5% errors. For (a), (b), and (c), the initial fidelity  $F_0$  is (i) 100% (ii) 99% (iii) 98% (iv) 97% (v) 96% with phase errors only. (b) Time scaling with distance for  $m=3$ , given in units of  $T_0 = (t_0 + t_c)/P$ , the time required to generate entanglement between nearest neighbors, and  $L_0$ , the distance between nearest neighbors. Measurement and local operation times are neglected. Note that the axes are logarithmic, so time scales polynomially with distance. (c) Long-distance asymptote dependence on initial fidelity for phase errors only. (d) Long-distance asymptote dependence on error type. For the calculations shown,  $F_0 = 0.99$ , and the shape parameter ranges from  $v = 0$  to  $v = 0.3$ .

protocol to the parameters of a desired implementation. Further speed-up may also be possible in the case when collection efficiency is very high by using coincidence detection in combination with e.g. time-bin encoding [1].

We conclude with two specific examples for potential implementation of the presented method. The nitrogen vacancy (NV) center in diamond has a strong, state-selective optical transition (Figure 3a) near 637nm which has been used for robust generation of single photons on demand [14, 15] and single spin measurement [21]. The triplet electron spin ground state is strongly coupled to a nearby  $^{13}\text{C}$  impurity nuclear spin, which can have a very long coherence time [25]. Spin selective fluorescence allows electron spin initialization, measurement [21] and entanglement with outgoing photons; electron spin resonance (ESR) and nuclear magnetic resonance (NMR) have already been employed to manipulate coupled electron and nuclear spins [23]. In the ground state, the energy splitting between electron spin states  $M_s = 0$  and  $M_s = \pm 1$  is an order of magnitude larger than the hy-

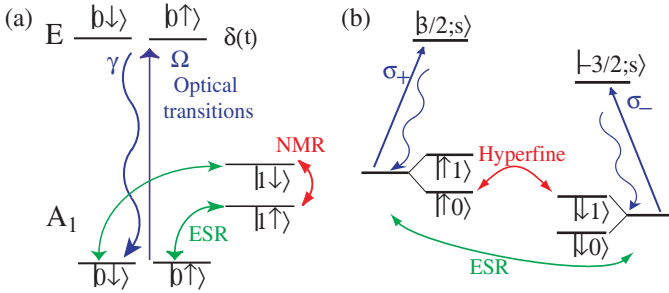


FIG. 3: Implementation with solid-state photon emitters. (a) Electronic ( $|0\rangle, |1\rangle$ ) and nuclear ( $|\uparrow\rangle, |\downarrow\rangle$ ) states of the NV center coupled to a  $^{13}\text{C}$  nuclear spin; their optical, microwave, and RF transitions. (b) Electronic ( $|\uparrow\rangle, |\downarrow\rangle$ ) and collective nuclear ( $|0\rangle, |1\rangle$ ) states and their transitions for singly doped quantum dots in a polarized nuclear spin lattice. To suppress background light scattering, two-photon excitation can be used in both cases.

perfine interaction, effectively decoupling the nuclear and electronic spin unless ESR and NMR pulses are applied. Since the optical transition frequency between states with  $M_s = 0$  is independent of nuclear spin state, information may be safely stored in the nuclear spin during light scattering. For NV centers coupled to cavities with Purcell factors  $\sim 10$ , [17] we find that the dominant source of error is electron spin decoherence during the classical communication period. Using an emission probability  $P_{\text{em}} \sim 5\%$ , a collection efficiency  $\epsilon \sim 0.2$ , and a classical communication time of  $t_c \sim 70\mu\text{s}$  over  $L_0 \sim 20$  km, we find the fidelity of directly entangled pairs can reach  $F_0 \sim 97\%$  for electron spin coherence times in the range of a few milliseconds. Electron spin coherence times in the range of  $100\mu\text{s}$  have been observed at room temperature and significant improvements are expected for high purity samples at low temperatures [26]. The large hyperfine splitting allows fast local operations between electron and nuclear spin degrees of freedom on a timescale  $\sim 100\text{ns}$  [23] much shorter than the decoherence time, allowing  $1 - p < 1\%$ . Finally, cavity enhanced collection should significantly improve observed measurement efficiencies of  $\eta \sim 80\%$  [23].

Semiconductor quantum dots [17] represent another promising physical implementation. By doping neutral dots with single electrons, the ground state of the dot contains an electron spin degree of freedom. This spin state has already been prepared and measured by state-selective optical transitions and all-optical Raman-based ESR in GaAs dots [27]. Hyperfine coupling of the electron spin to the surrounding lattice of nuclear spins allows nuclear polarization and use of collective nuclear spin excitations as a quantum memory [28] with potential coherence times on the order of seconds [25]. Although optical transitions in doped quantum dots can exhibit homogeneous broadening  $\Gamma \sim 100 \text{ GHz} \sim 10 - 100\gamma$  [29], the corresponding error can be made negligible by send-

ing the output from the cavity through a frequency filter with a linewidth of a few hundred MHz. Assuming a high degree of nuclear spin polarization ( $P_n \gtrsim 0.95$ ) [27] and active ESR pulse correction, electron spin dephasing is expected to be in the ms range [30].

In conclusion, we have shown that by combining these state-of-the-art quantum optical emitters in the solid state with techniques for electron and nuclear spin manipulation, quantum communication over long distances can be achieved. Potential applications may include, for instance, secure transmission of secret messages over intercontinental distances.

The authors wish to thank Phillip Hemmer, Aryesh Mukherjee, Alexander Zibrov, and Gurudev Dutt. This work is supported by DARPA, NSF, ARO-MURI, and the Packard, Sloan and Hertz Foundations and the Danish Natural Science Research Council.

---

- [1] W. T. N. Gisin, G. Riborty and H. Zbinden, Rev. Mod. Phys **74**, 145 (2002).
- [2] G. Brassard, N. Lutkenhaus, T. More, and B. Sanders, Phys. Rev. Lett. **85**, 1330 (2000).
- [3] H. J. Briegel, W. Dur, J. I. Cirac, and P. Zoller, Phys. Rev. Lett. **81**, 5932 (1998).
- [4] M. Zukowski *et al.*, Phys. Rev. Lett. **71**, 4287 (1993).
- [5] Bennett, C.H. *et al.*, Phys. Rev. Lett. **70**, 1895 (1993).
- [6] D. Bouwmeester *et al.*, Nature **390**, 575 (1997).
- [7] A. Ekert, Phys. Rev. Lett. **67**, 661 (1991).
- [8] C. Bennett *et al.*, Phys. Rev. Lett. **76**, 722 (1996).
- [9] D. Deutsch *et al.*, Phys. Rev. Lett. **77**, 2818 (1996).
- [10] B. Blinov *et al.*, Nature **428**, 153 (2004).
- [11] S. J. van Enk, J. I. Cirac, and P. Zoller, Science **279**, 205 (1998).
- [12] L. M. Duan, M. D. Lukin, J. I. Cirac, and P. Zoller, Nature **414**, 413 (2001).
- [13] J. McKeever *et al.*, Science **303**, 1992 (2004).
- [14] C. Kurtsiefer, S. Mayer, P. Zarda, and H. Weinfurter, Phys. Rev. Lett. **85**, 290 (2000).
- [15] A. Beveratos *et al.*, Phys. Rev. Lett. **89**, 187901 (2002).
- [16] P. Michler *et al.*, Science **290**, 2282 (2000).
- [17] C. Santori *et al.*, Nature **419**, 594 (2002).
- [18] C. Cabrillo, J. Cirac, P. Garcia-Fernandez, and P. Zoller, Phys. Rev. A **59**, 1025 (1999).
- [19] A. Muller *et al.*, Appl. Phys. Lett. **70**, 793 (1997).
- [20] L. Childress *et al.*, in preparation.
- [21] F. Jelezko *et al.*, Phys. Rev. Lett. **92**, 076401 (2004).
- [22] J. M. Taylor *et al.*, e-print: cond-mat/0407640 (2004).
- [23] F. Jelezko *et al.*, Phys. Rev. Lett. **93**, 130501 (2004).
- [24] W. Dur, H. J. Briegel, J. I. Cirac, and P. Zoller, Phys. Rev. A **59**, 169 (1999).
- [25] C. Ramanathan *et al*, eprint: quant-ph/0408166 (2004).
- [26] T. Kennedy *et al.*, Appl. Phys. Lett. **83**, 4190 (2003).
- [27] A. S. Bracker *et al.*, e-print:cond-mat/0408466 (2004).
- [28] J. M. Taylor, C. M. Marcus, and M. D. Lukin, Phys. Rev. Lett. **90**, 206803 (2003).
- [29] A. Kiraz *et al.*, Phys. Rev. B **65**, 161303(R) (2002).
- [30] V. Golovach, A. Khaetskii, and D. Loss, eprint: cond-mat/0310655 (2003).